PAPER

Check for updates

Navigating materials design spaces with efficient Bayesian optimization: a case study in functionalized nanoporous materials

Panagiotis Krokidas, [ID] *[a] Vassilis Gkatsis, [ID] †[ab] John Theocharis [ID] †[c] and George Giannakopoulos [ID] [ad]

Machine learning (ML) has the potential to accelerate the discovery of high-performance materials by learning complex structure–property relationships and prioritizing candidates for costly experiments or simulations. However, ML efficiency is often offset by the need for large, high-quality training datasets, motivating strategies that intelligently select the most informative samples. Here, we formulate the search for top-performing functionalized nanoporous materials (metal–organic and covalent–organic frameworks) as a global optimization problem and apply Bayesian Optimization (BO) to identify regions of interest and rank candidates with minimal evaluations. We highlight the importance of a proper and efficient initialization scheme of the BO process, and we demonstrate how BO-acquired samples can also be used to train an XGBoost regression predictive model that can further enrich the efficient mapping of the region of high performing instances of the design space. Across multiple literature-derived adsorption and diffusion datasets containing thousands of structures, our BO framework identifies 2×- to 3×-more materials within a top-100 or top-10 ranking list, than random-sampling-based ML pipelines, and it achieves significantly higher ranking quality. Moreover, the surrogate enrichment strategy further boosts top-N recovery while maintaining high ranking fidelity. By shifting the evaluation focus from average predictive metrics (*e.g.*, R^2, MSE) to task-specific criteria (*e.g.*, recall@N and nDCG), our approach offers a practical, data-efficient, and computationally accessible route to guide experimental and computational campaigns toward the most promising materials.

1 Introduction

The advent of Machine Learning (ML) has introduced powerful capabilities in the discovery and development of novel materials,[1] particularly through its ability to uncover complex structure–property relationships. In this context, ML models can learn to map structural and chemical information to macroscopic material properties, enabling fast and efficient predictions. As a result, experimental or computationally expensive methods can be reserved for only the most promising candidates. In the field of functionalized nanoporous materials, recent studies have showcased the potential of artificial intelligence—from conventional ML models capable of high-accuracy property prediction,[2,3] to emerging approaches based

on Large Language Models (LLMs),[4,5] and generative models capable of proposing entirely new material structures.[6]

Despite these advances, ML-driven discovery remains constrained by several challenges. Chief among them is the paradox between the promise of ML to reduce experimental costs and the substantial data requirements it imposes. Generating sufficiently large, high-quality datasets—whether through experiments or simulations—can be prohibitively expensive, undermining the very efficiency ML aims to deliver.[7–9] To address this, significant effort has been invested in smart sampling strategies, broadly referred to as Active Learning (AL),[10,11] which aim to minimize the number of required samples while maximizing predictive accuracy.

However, despite their conceptual appeal, many AL strategies often struggle to consistently outperform passive learning approaches,[12] in which ML models are trained on randomly selected samples. In fact, random sampling remains a surprisingly strong benchmark.[11] Moreover, maximizing predictive performance (*e.g.*, *via* R^2, mean squared error) may not always align with the practical goals of materials scientists. In many cases, the primary objective is not to model the entire design space, but rather to identify regions containing top-performing

[a]Institute of Informatics and Telecommunications, National Centre for Scientific Research "Demokritos", Agia Paraskevi, 15310, Greece. E-mail: p.krokidas@iit.demokritos.gr

[b]Department of Informatics and Telecommunications, National and Kapodistrian University, Athens, Greece

[c]Physics Department, National and Kapodistrian University, Athens, Greece

[d]SciFY PNPC, Athens, Greece

† These authors contributed equally to this work.

materials. As we demonstrate in this work, standard ML metrics often fail to reflect performance in this specific task.

Identifying high-performing sub-regions can be formulated as an optimization problem in which a sampling algorithm iteratively selects new points, not to reduce uncertainty as in active learning, but to maximize an acquisition function. An acquisition function is a heuristic that quantifies the utility of evaluating a candidate point, balancing exploration of uncertain regions with exploitation of high-predicted-value regions. Bayesian Optimization (BO) provides a principled solution in this context, serving as a global optimizer over complex design spaces.[13–16] In this work, we adapt BO not only to identify the single best-performing instance, but also to recover an ensemble of the top-N performers (*e.g.*, top-10 or top-100), reflecting the practical needs of materials scientists who often require multiple candidates rather than a solitary optimum. We address the following core research questions:

(1) How many samples are needed to identify regions within large design spaces (containing thousands to hundreds of thousands of materials) that contain top-performing candidates? We note that this number depends strongly on the task at hand, the complexity of the underlying structure–property relationships, and the choice of feature representation.

(2) How many samples are required to identify the single best-performing material in such spaces?

(3) How does our approach compare to an ML model trained on an equal number of randomly selected samples, particularly in terms of ranking the top-performing materials and identifying the global optimum?

While BO is a powerful framework, it can incur substantial computational expense.[17] To mitigate this, we introduce frugality-oriented elements. Here, frugality refers primarily to minimizing the number of costly experimental or simulation evaluations required to identify high-performing materials, which is the main bottleneck, but we also consider simple strategies to reduce computational overhead. First, we quantify how the choice of initial samples influences BO's convergence and overall performance. Unlike our baseline method (Random Sampling ML), BO is always initialized with a simple yet effective, informed strategy that combines one central point and two diverse points, ensuring both representativeness and diversity in the initial sampling. This primarily supports experimental efficiency by ensuring informative early evaluations. Next, we evaluate batch sampling strategies—selecting multiple candidates per iteration—to strike an optimal balance between predictive accuracy and runtime efficiency. Batching reduces computational cost by limiting the number of surrogate retrainings, while also enabling parallel experiments in principle. Finally, we show that, by training a machine-learning surrogate (*e.g.*, XGBoost) on the BO-acquired samples after the campaign, we can predict and rank the remainder of the design space. This enrichment step mainly reduces experimental effort by identifying additional top-N candidates without further evaluations, while also providing a lightweight ranking at low computational cost. Fig. 1 summarizes our approach.

We evaluate our method across a diverse collection of literature-based datasets involving gas adsorption and diffusion in functionalized nanoporous materials, including metal–organic frameworks (MOFs) and covalent–organic frameworks (COFs). In all cases, our BO framework outperforms random-sampling-based ML pipelines in both identifying and ranking top-performing candidates. Notably, we not only measure success in terms of top-performer recovery but also assess the quality of the ranking (nDCG; see Section 2.4).

2 Methodology

2.1 The premise

As outlined in the introduction, the premise of this work is that researchers in a laboratory often operate within a specific experimental budget while seeking the best or top-performing materials from a vast design space of nanoporous materials. Typically, this budget, represented by N (the number of new materials evaluated), is significantly smaller than the total number of materials available in the design space ($N \ll N'$, where N' denotes the total number of available materials). Consequently, identifying the best or top-performing materials by randomly selecting and testing N samples relies purely on
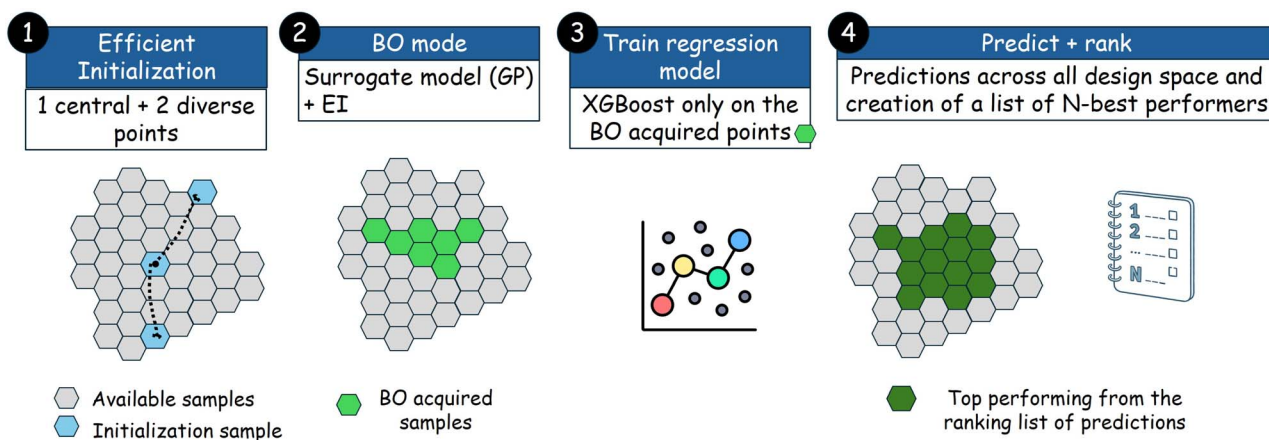

Fig. 1 Pipeline of the Bayesian optimization method in this work.

chance. ML offers an alternative: it can use these N randomly selected samples to train a model, predict performance across the entire design space, and rank all available materials based on predicted performance.

Inspired by recent advancements in Bayesian Optimization (BO) applied to MOFs and related materials, we investigate the potential of BO to guide researchers in allocating their N experiments. The goal is to iteratively direct experiments toward regions of the design space with higher performance, progressively converging on areas of interest and improving efficiency in identifying exceptional materials.

2.2 Problem formulation

Suppose a set M containing all nanoporous materials $m \in M$. Each material m can be uniquely identified by a set of n feature properties f (hereby called features). Each point in this multi-dimensional $\mathbb{R}^n$ space corresponds to the design of one material and each material may differ slightly or greatly from the others in terms of a target property value. So:

$$m_i \in M \subset \mathbb{R}^n, \quad m_i = \{f_1, \ f_2, ..., \ f_n\} \tag{1}$$

We define a machine learning model as the process p that learns the mapping from the general material space $\mathbb{R}^n$ to this target property y, so:

$$p : \mathbb{R}^n \to \mathbb{R} \tag{2}$$

Let the dataset used to train this machine learning model be denoted as D_{train} which consists of N data points, same as the budget for experiments. This can be defined as:

$$D_{\text{train}} = \left\{ (x_j, y_j) \big| x_j \in \mathbb{R}^n, \ y_j \ \text{in} \ \mathbb{R}, \ j = 1, 2, ...n \right\} \tag{3}$$

Similarly we can define the test dataset D_{test} and the evaluation dataset D_{eval}. Now lets consider a method for evaluating this model. Let us denote this method as $\mathcal{E}(p, D_{\text{eval}})$ which takes the ML model p and evaluation dataset and provides a measure of the performance of the model. The logic and metrics used for the evaluation are described in detail in the Evaluation metrics section.

Our goal is to use the least amount of data, less than or equal to the available budget, in order to achieve the best performance score. In practical terms, this problem is inherently multi-objective: we aim to minimize the number of samples required for training while simultaneously maximizing the predictive performance of the model. The trade-off between these two goals is the central question addressed in this work.

2.3 AI methodologies

2.3.1 The conventional ML way: random sampling, train and predict. The popular approach of employing data-guided methodologies in cases of unsolved complex correlations in novel materials design is, given the existence of a design space of input structural and chemical parameters, choose a sub-set of them, label them (*e.g.* measure the desired target property value for each of them) through expensive experiments or simulations, and use the results as a dataset to train an ML regression model to predict the property values for the rest of the design space. We refer to this as the random way. In our work, for the sake of sufficient statistical evaluation we repeat the procedure 20 times, varying the data sampled. As our main model we have selected XGBoost[18] due to its efficiency on regression tasks. More details on the specifics of the XGBoost in our work can be found in the SI.

2.3.2 Bayesian optimization. The basic block of this project is the Bayesian Optimization (BO) process, which, as the name suggests, is a method to optimize (find maxima or minima) of an unknown function. As mentioned in the Problem formulation section, an ML model can be described as a function mapping inputs (features) to outputs (target property values). The underlying structure–property relationship that we seek to approximate is usually referred to as a "black box", since in most cases it cannot be expressed with a closed formula. The ML model provides an explicit approximation to this black-box mapping. In this way, BO becomes an efficient method for guiding the search toward maxima or minima of the property of interest.

BO is an iterative process where at each iteration we train an ML model (called a surrogate model) with the currently acquired data, we use this model to make predictions about a specific data property on the whole dataset. Finally an acquisition function is being utilized to select the most informative data point and add it to the dataset. The surrogate's uncertainty quantification is central to this process, since the acquisition function balances exploration (sampling uncertain regions) with exploitation (sampling high-predicted-value regions). Practically, the surrogate model represents our current beliefs about the target property that we are trying to maximize (or minimize) and the acquisition function seeks to select data points from areas of the data space that we lack knowledge of. By transferring this scheme to our problem, we state that BO determines which experiments should be performed by designating the most promising candidate materials in terms of target property value maximization.

We adopt the open-source implementation of Gantzler *et al.*,[19] which is built on the BoTorch library[20] for Gaussian process–based Bayesian optimization, as the foundation for our framework; in Section 2.5, we detail the extensions we introduce on top of this BO implementation.

In the following paragraph we make clarifications concerning the details of our method.

As our surrogate model we have selected a Gaussian Process (GP) model due to its efficiency in representing the uncertainty of knowledge. The model consists of two parts, a mean function and a kernel (covariance function)

$$Y(x) \sim \text{GP}(\mu(x), K(x, x')) \tag{4}$$

In our case as a mean we have used a constant mean function

$$\mu(x) = C \tag{5}$$

and squared exponential (or Radial Basis Function RBF) as our kernel which is defined as

$$K\left(x, x'\right) = \exp\left(-\frac{1}{2}(x - x')^T \Theta^{-2}(x - x')\right) \quad (6)$$

Both C and Θ are parameters that are calculated automatically by the SingleTaskGP model contained in the BoTorch library.

The acquisition function that we have selected is Expected Improvement (EI):

$$\operatorname*{argmax}_{x \in X} E[\max[0, Y(x) - y^*]] \quad (7)$$

where $Y(x)$ represents our current prediction of target property at point x in the design space, and y^* is the maximum observed target property value so far. EI balances exploration and exploitation by favoring either points with high predicted values or those with high model uncertainty. It is worth noting that EI and related acquisition functions have also been extended to multiobjective problems, often under the name of Efficient Global Optimization (EGO). These methods adapt EI to identify Pareto-optimal fronts or high-performing regions in multi-objective spaces, and have seen significant use in cheminformatics and materials discovery.[19,21] While in this work we restrict our focus to single-objective optimization, these connections are relevant for readers interested in multiobjective extensions.

At the conclusion of the BO process, users gain access to a curated set of high-performing materials from the design space. As we will demonstrate later, these selected points form an information-rich dataset containing instances of optimal performance. This dataset can then be used to train the same predictive model employed in the random sampling approach (XGBoost), enabling it to make predictions across the entire design space and further expand the list of high-performing materials with additional suggested candidates. Consequently, the final selection of top-performing materials is derived from a combined dataset consisting of BO-acquired samples and XGBoost predictions trained exclusively on these samples. As we will show in later sections, this strategy proves highly effective, as the trained model excels at distinguishing and identifying high-performing instances, further enhancing the optimization process. A graphical representation of our pipeline is depicted on Fig. 1.

Recent works have applied BO directly to nanoporous materials design. Deshwal *et al.*[22] demonstrated that BO can efficiently navigate a database of 70 000 COFs to identify those with highest methane deliverable capacity, outperforming random search, evolutionary algorithms, and one-shot ML baselines, while also acquiring a significant fraction of the top-performing structures after relatively few evaluations. Gantzler *et al.*[19] extended this idea by employing multi-fidelity BO for COFs in Xe/Kr separations, showing that combining low-cost approximate evaluations with high-fidelity simulations accelerates the search. Together, these studies established BO as a powerful framework for adsorption and diffusion problems in porous materials. In this work, we demonstrate how three complementary elements—diversity-preserving initialization,

batch-mode acquisitions, and surrogate enrichment with XGBoost—can be combined into a coherent framework, whose integration provides a practical and effective workflow for materials discovery.

2.4 Evaluation metrics

We trained and evaluated our regressor across the various training dataset sizes that will be presented in a following section, aiming to determine the minimum number of training samples required to effectively capture the most promising region of the design space in terms of target property maximization. In this section, we define what constitutes a promising area and outline the evaluation metrics used to assess our machine learning model's ability to identify it.

In our experiments, where the design space is finite and the target property values for all candidate materials are known, we can easily rank the materials in descending order and extract the top-N (where N is either 100 or 10, in this work). Ideally, our model's predictions should rank the same materials within the top-N while closely approximating their actual target property values. To evaluate our model's performance in these tasks, we employed the following metrics.

2.4.1 Recall@N. Recall@N is the proportion of relevant items found within the top-N predicted, where N in this work is either 100 or 10, depending on the case under study:

$$\text{Recall@}N = \frac{\text{predicted on top-}N}{\text{actuall top-}N} \quad (8)$$

This measure is the simplest way to acknowledge whether our trained model can correctly identify promising materials, without giving any importance on the predicted target property value or the actual ranking of the correctly predicted materials. A model with high Recall@N score would be useful for experimental scientists working on largely unknown datasets where it is more important to find several promising candidates rather than only the single best one.

2.4.2 Mean percentage error. Mean Percentage Error (MPE) is defined as:

$$\frac{N}{n} \sum_{i=1}^{n} \frac{|\text{pred}_i - \text{actual}_i|}{\text{actual}_i} \quad (9)$$

In our case we measure MPE on the predicted top-N so n is the number of materials correctly predicted to belong to the actual top-N on the dataset, pred_n is the predicted target property value of nth material and actual_n is the actual value. This metric gives us a notion of how close (in percentage terms) is our model at predicting the values of top-N materials, and it is useful in scenarios where knowing the exact target property value is crucial.

2.4.3 Normalized discounted cumulative gain. Normalized Discounted Cumulative Gain (nDCG)[23] is a measure which compares the quality of a proposed ranking in accordance to an ideal ranking by giving emphasis on the correct identification of higher valued items. The mathematical formula is:

$$\text{nDCG}_p = \frac{\text{DCG}_p}{\text{iDCG}_p} \quad (10)$$

where DCG_p is the discounted cumulative gain and $iDCG_p$ is the same measure for the ideal ranking which can be expressed as:

$$iDCG_p = \sum_{i=1}^{|REL_p|} \frac{2^{rel_i} - 1}{\log_2(i + 1)} \tag{11}$$

p is the number of items involved in the ranking. So, in a case where $N = 100$, we measure the top-100 ranking so $|REL_p| = 100$, and rel_i is a relevance score given to each item in the ranking based on how important it is considered to be higher. So in our case where we have $n > 100$ candidate materials and we want to find the top-100 the relevance of each material would be in descending order from 100 to 1 and 0 for each one that should not be in the top-100. Thus the material relevance pairs are in the form (x_i, rel_i)

$$\begin{aligned} &(x_1, 100), (x_2, 99), (x_3, 98), \ldots, (x_{99}, 2), \\ &(x_{100}, 1), (x_{101}, 0), (x_{102}, 0), \ldots, (x_n, 0) \end{aligned} \tag{12}$$

2.5 Beyond baseline BO: practical additions

In this section, we summarize a set of additions to standard Bayesian optimization. Some of these strategies (*e.g.*, diverse initialization, batch acquisitions) have appeared in the literature, while others (*e.g.*, enrichment of BO findings with predictions) are introduced here. Taken together, they provide a clear improvement in efficiency and make our BO framework more practical for materials discovery. We present them as recommended extensions that practitioners may find useful when applying BO to large design spaces.

2.5.1 Enriching BO findings with predictions. As previously discussed, the outcomes of the BO procedure are further expanded by training an XGBoost model on the BO-acquired samples. This model is then used to predict the target property across the remaining, unlabeled design space. By ranking the top-N predicted materials, we obtain an enriched and more complete list of high-performing candidates, extending the reach of the original BO search.

2.5.2 Efficient initilization. To initialize the Bayesian Optimization (BO) process, an initial set of data points must be selected. In many studies, this is achieved by randomly sampling a subset of the design space, which then serves as the starting dataset for the surrogate model. For example, Deshwal *et al.*[22] adopted this approach by randomly selecting three covalent organic frameworks (COFs) from their dataset to initialize the BO loop.

However, purely random initialization can introduce statistical variability, potentially leading to inconsistencies in performance when applying BO to real-case scenarios. To mitigate this, in our work we employ an informed initialization strategy rather than random selection, following the approach of Gantzler *et al.*[19] Specifically, we first determine a central sample by computing the mean of all feature values and selecting the candidate whose features are closest to this mean, which serves as a representative point of the design space. Next, to ensure diversity in the initial training set, we apply a diverse-set selection procedure that, starting with the central sample, iteratively identifies additional samples that maximize the minimum Euclidean distance from the already selected points.

This procedure guarantees that the initial three samples are simultaneously representative and diverse, providing the Gaussian process surrogate model with a robust starting dataset for BO. In our case, three such samples were selected. As shown in the SI (Table S1), this approach yields performance comparable to the average of 20 BO runs with different random initializations (three points each, 100 steps), in identifying the top-100 instances for all datasets considered in this work. We emphasize that this comparison was performed deliberately to confirm that our initialization scheme does not bias performance upward relative to random initialization, but rather offers a practical and robust one-shot alternative in settings where repeated BO restarts are not feasible.

We note that the notion of 'diversity' depends on the chosen feature representation; different fingerprints (*e.g.*, chemical *vs.* geometric) can yield different diverse sets.[24] The present work adopts the feature sets provided in the literature datasets considered here, but in general, the effectiveness of a diversity-based initialization strategy depends on the availability of a feature representation that meaningfully captures structural and chemical differences.

2.5.3 Batch sampling for faster BO calculations. Bayesian Optimization (BO) is computationally expensive, particularly when applied to large design spaces or at high sampling rates. This is primarily due to the need to invert the covariance matrix of the Gaussian Process (GP) regressor, an operation that scales with $O(n^3)$ complexity,[17] where n is the sample size. In standard BO, each newly selected sample requires retraining the GP model to determine the next sampling point. To alleviate this burden, we employed batch sampling: instead of retraining the surrogate model after each sample, we updated it only once per batch, following the evaluation of all batch points. This significantly reduced the number of surrogate model updates and the associated computational cost—most notably by limiting the number of expensive covariance matrix inversions. Sequential BO is optimal in terms of information gain per sample. Batch BO, however, trades off some of this efficiency for practical gains: fewer retrainings of the surrogate and the ability to parallelize evaluations. As such, modest batch sizes (*e.g.* 5) achieve nearly the same recall@N as sequential BO, but in significantly less wall-clock time, representing a practical compromise.

Fig. S1 in the SI compares single-sample BO with batch sizes of 5 and 10 samples per iteration, evaluating their performance in terms of recall@100 and best-sample identification as functions of sample size and computational time. The test case involves the dataset by Mercado *et al.*,[25] comprising 70 000 COFs evaluated for methane deliverable capacity. Based on this analysis, we adopt a batch size of 5 samples per BO iteration throughout this work, as it provides an effective balance between computational efficiency and performance. Notably, this configuration achieves the same recall@100 and identifies the best-performing COF using 700 samples at just one-tenth of the computational time compared to single sampling. We note that batch BO itself is well established in the literature,

particularly through methods such as q-EI.[26,27] Here, we adopt a simpler strategy: selecting the top-k EI points per iteration. This makes batching straightforward to implement in similar workflows while retaining the benefits of parallelism and reduced runtime.

Fig. 1 summarizes our approach, as was described in Section 2.5.1–2.5.3.

2.6 Datasets

In this section we summarize all the datasets used in this work. Mercado et al.[25] reported a database of approx. 70 000 COF, where they report the uptake and deliverable capacity of CH_4 in them, through Monte Carlo simulations. The same COFs database was used by Deshwal et al.,[22] for methane uptake values, for the development of a BO routine that identifies the best candidate material. The same structure database was employed in the 2023 work by Aksu and Keskin[2] for where they report a high-throughput and ML scheme for the identification of COFs with CH_4/H_2 separation performance. Here, we use CH_4 uptake and deliverable capacity as target values. Orhan et al.[28] reported a 5600 MOFs databases in their high throughput screening work for O_2/N_2 materials. The target properties we considered were the diffusivity and uptake of O_2, and the diffusion selectivity of O_2/N_2. Another database we considered was the one developed by Majumdar et al.[29] which includes more than 20 000 hypothetical MOFs, along with various gas properties, of which we kept H_2 uptake capacity, CO_2 uptake, N_2 uptake, CO_2 working capacity, and CO_2/N_2 selectivity. This database was employed, also, by Daoo et al.[30] in their work on Active Learning methods for high-performing MOFs for the separation of C_2H_2/C_2H_4 and C_3H_6/C_3H_8. We kept as target properties the C_2H_2 and C_2H_4 uptakes. Villajos et al. in their 2023 work[31] reported an extended dataset for H_2 adsorption at cryogenic temperatures, where they provide 3600 MOFs with crystallographic and porous properties, along with volumetric and gravimetric capacities. In our work we consider as target property the gravimetric capacity. Aksu and Keskin[2] reported a high-throughput computational screening combined with ML for the identification of high-performing COFs as adsorbents for CH_4/H_2 separations in pressure-swing and vacuum-swing adsorption (PSA and VSA, respectively). In our work we considered as target properties the CH_4 and H_2 uptakes at 1 bar pressure.

3 Results and discussion

3.1 A first demonstration case for a fixed number of 100 samples: "COFs with high deliverable capacity as target property" as a testbed of comparison"

In this section, we evaluate our BO approach using the methane deliverable capacity dataset from Mercado et al.[25] as a testbed. We compare our method against a conventional ML approach in the context of a lab operating on a limited budget of 100 samples.

3.1.1 Traditional approach – Random Sampling ML. We randomly select 100 COFs and their corresponding methane deliverable capacity values as a training set for an XGBoost

regressor. This predictive model is then used to estimate the methane deliverable capacity for all remaining COFs in the dataset.

3.1.2 BO approach. We perform 100 BO iterations to focus on regions of the design space with high deliverable capacity. The 100 COFs acquired through BO, along with their methane deliverable capacity values, are used to train an XGBoost
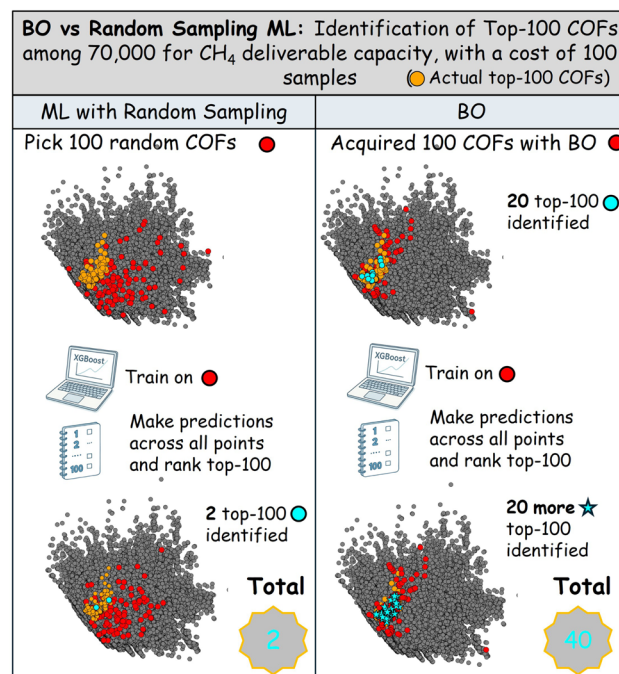

Fig. 2 Pipeline of identifying top-performing COFs (in terms of methane deliverable capacity) in a design space of 70 000 COFs with a ML model trained on 100 random samples, and our BO methodology: the randomly trained ML identifies correct only 2 COFs belonging to the top-100 performing ones, while our BO approach identifies 40.
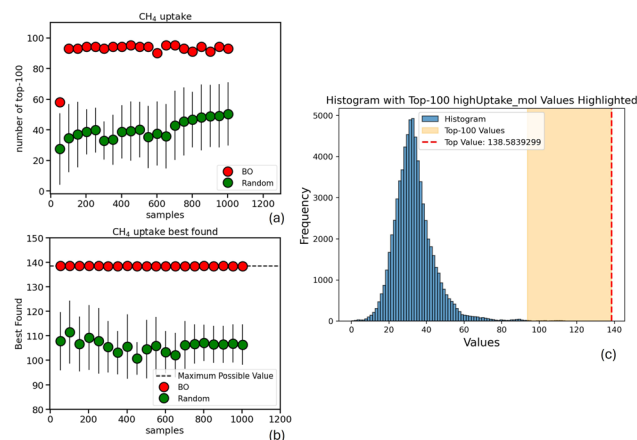

Fig. 3 Comparison of Bayesian Optimization (BO) and Random Sampling ML at identifying the (a) top-100 COFs and (b) overall best COF for methane uptake, as a function of sample size; (c) distribution of methane uptake values in the whole dataset (yellow area denotes the top-100 COFs and dash red line the sole best COF).
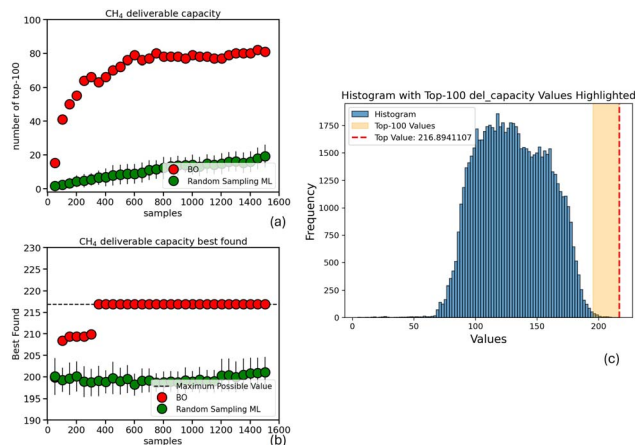
Fig. 4 Comparison of Bayesian Optimization (BO) and Random Sampling ML at identifying the (a) top-100 COFs and (b) overall best COF for methane deliverable capacity, as a function of sample size; (c) distribution of deliverable capacity values in the whole dataset (yellow area denotes the top-100 COFs and dash red line the sole best COF).

regressor. This model is subsequently used to predict the deliverable capacity for the rest of the COFs.

A ranking of the top-100 predicted values compared with the actual top-100 reveals that the conventional ML (Random Sampling ML) approach identifies only 2 of the true top-100 performing COFs. In contrast, the BO approach successfully selects 20 COFs within the top-100 tier. Moreover, when the XGBoost model is trained on the BO-acquired samples, it identifies an additional 20 top-performing COFs, boosting the overall count to 40.

This result highlights the value of using Bayesian Optimization (BO) to acquire high-interest samples, as it complements and enhances subsequent ML-based ranking. Although the XGBoost model trained on BO-acquired samples exhibits lower overall predictive performance—achieving an R^2 of 0.70 compared to 0.85 for the model trained on randomly selected samples, along with a higher MSE (see Fig. S2 in the SI)—its focused training on a promising subregion of the design space makes it particularly effective at accurately identifying and ranking the top-performing COFs.
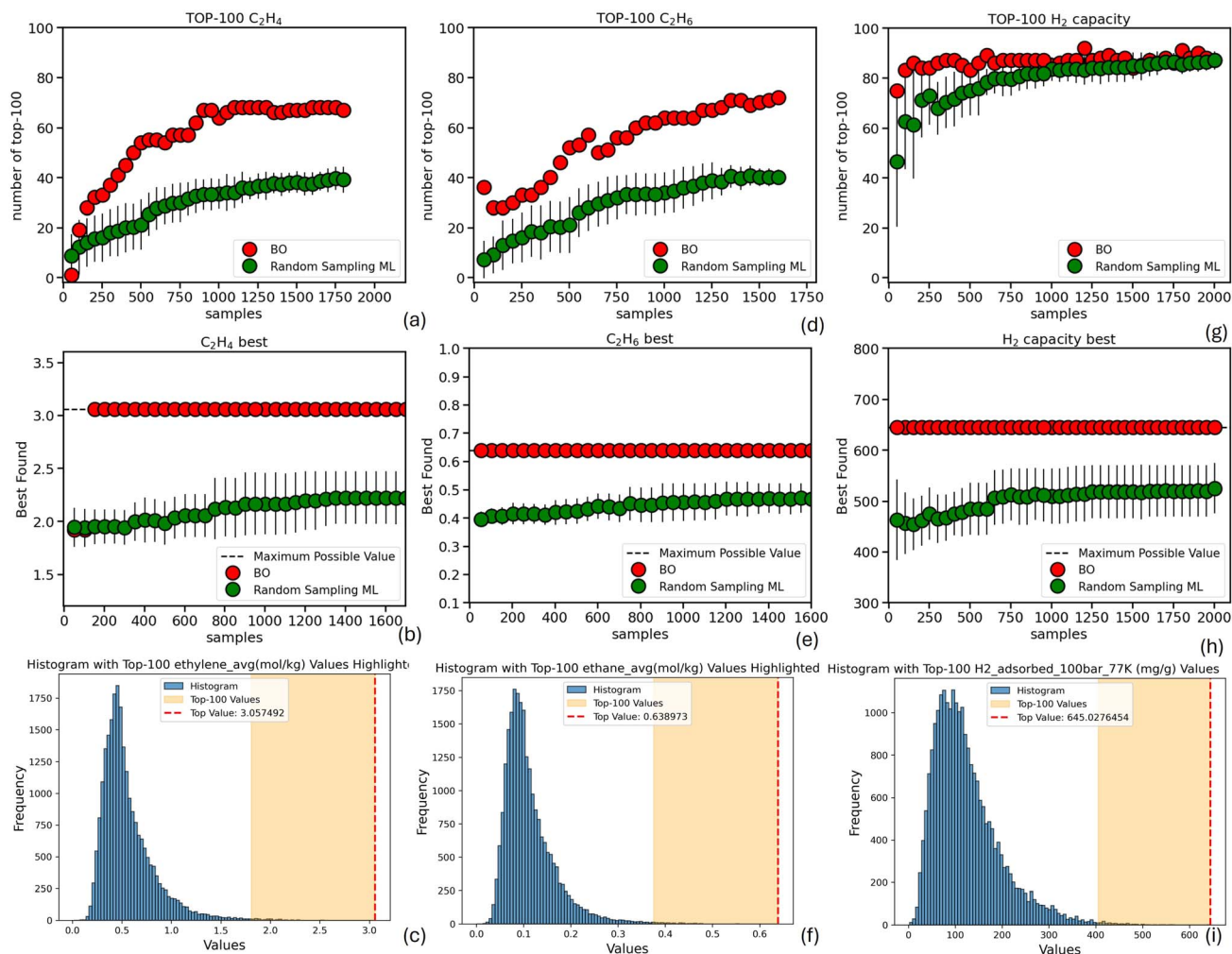

Fig. 5 Comparison of Bayesian Optimization (BO) and Random Sampling ML across three target properties: ethylene ((a)–(c)), ethane ((d)–(f)), and hydrogen uptake ((g)–(i)). (top row) Number of top-100 performing materials identified as a function of sample size. (middle row) Number of samples required to identify the top-1 performing material. (bottom row) Distribution of target property values across each dataset, providing context on the difficulty of each search task. Each plot compares the performance of BO and random sampling, illustrating the relative effectiveness of each approach in different regimes.

This becomes evident when evaluating the models specifically on the top-100 region: the XGBoost model trained on BO-selected samples achieves better R^2 and lower MSE than the one trained on random samples Fig. S2, despite its lower global metrics. This illustrates that common evaluation metrics such as R^2 and MSE, when applied over the entire dataset or random subsets, can be misleading in assessing a model's true utility. In scenarios where the goal is to discover rare but high-value regions in the design space, average performance across the whole dataset does not reflect the model's effectiveness in those critical areas.

Thus, our approach uses BO for targeted sample acquisition in a large design space and then employs ML to enrich the top-100 findings, through predictions (Fig. 2).

3.2 All dataset results

In this section, we apply our BO approach and benchmark it against the Random Sampling ML baseline across all literature datasets introduced in the Methodology section. The comparison is carried out as a function of the evaluation budget, ranging from 1000 to 2000 sample evaluations. Performance is assessed in terms of the top-100 or top-10 candidates identified (depending on the design space size), as well as the single best material discovered, each reported as a function of the available evaluation budget.

First, we evaluate the methane uptake dataset for COFs from Mercado et al.[25] As shown in Fig. 3(a), although the XGBoost model trained on randomly selected samples (Random Sampling ML) gradually improves its recall@100 with increasing sample size, even 1000 samples yield only marginal gains (recall@100 ≈ 50). In stark contrast, our BO framework achieves a recall@100 of 93 from the very first iterations. Remarkably, BO pinpoints the single best-performing COF with just 50 samples, whereas the random sampling strategy fails to identify the top candidate even after 1000 evaluations.

Moreover, it is worth mentioning that the nDCG values are considerably higher for BO, highlighting the ability of our approach to not only find more of the top-100 instances, but ensure a more accurate positioning of them, closer to the actual
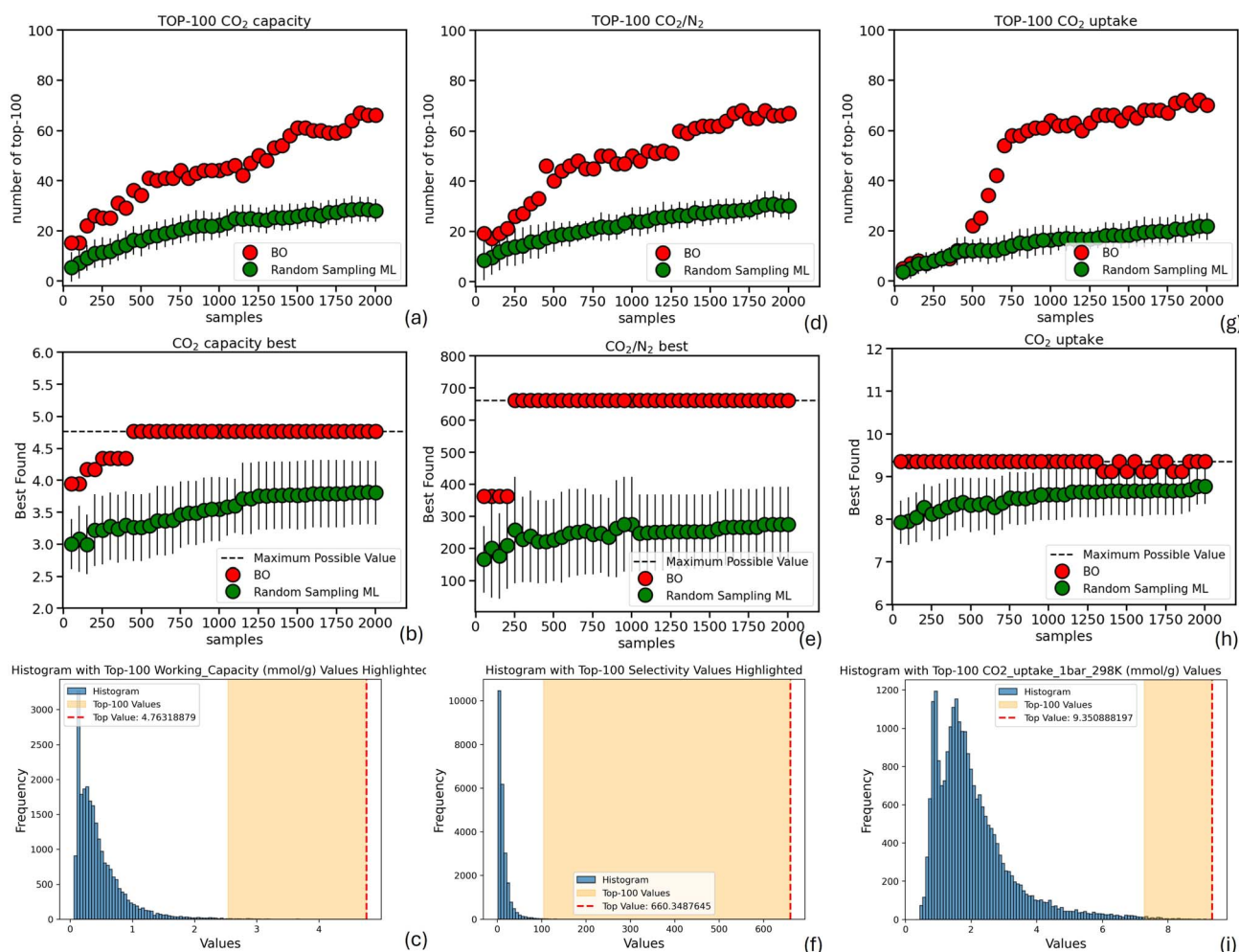

Fig. 6 Comparison of Bayesian Optimization (BO) and Random Sampling ML across three target properties: CO_2 working capacity ((a)–(c)), CO_2/N_2 ((d)–(f)), and CO_2 uptake ((g)–(i)). (top row) Number of top-100 performing materials identified as a function of sample size. (middle row) Number of samples required to identify the top-1 performing material. (bottom row) Distribution of target property values across each dataset, providing context on the difficulty of each search task. Each plot compares the performance of BO and random sampling, illustrating the relative effectiveness of each approach in different regimes.

ranks of the materials, in terms of their performance (see Fig. S3).

Fig. 4(a) demonstrates that for the more challenging methane deliverable capacity target, BO still vastly outperforms the conventional ML approach based on Random Sampling ML in terms of recall@100. The BO approach identifies up to 80 of the top-100 COFs—slightly lower than the performance for methane uptake—that creates a clear performance gap with the Random Sampling ML, which at 1500 samples identifies 19 top-100. This highlights BO's superior ability to target high-interest regions in complex design spaces.

Fig. 4(b) further emphasizes this advantage when it comes to identifying the single best-performing COF. For methane deliverable capacity, BO requires approximately 300 samples to reliably pinpoint the best COF, compared to just 50 samples for methane uptake. In contrast, the Random Sampling ML approach shows a steady but limited improvement in the best COF value as more samples are added, indicating its difficulty in effectively exploiting additional data to locate the optimum.

Moreover, nDCG is consistently higher for BO, reaching almost 1, while Random Sampling ML maxes below 0.9 (Fig. S3). These results confirm that BO is a highly effective sampling strategy, particularly in challenging scenarios where the design space is vast and the optimal regions are hard to exploit using conventional methods.

Fig. 5–7 summarize the results for the remaining datasets considered in this work. The first two columns of Fig. 5 illustrate the number of samples required by both Bayesian Optimization (BO) and Random Sampling ML to identify the top-100 and top-1 performing MOFs for ethylene and ethane uptake, respectively, based on the dataset from Daoo and Singh.[30] It is evident that, in both cases, BO successfully identifies significantly more of the top-100 performing materials with the same number of samples. Furthermore, BO is able to identify the single best-performing MOF within the very first steps, whereas Random Sampling ML exhibits only marginal improvements throughout the search (up to 1600 samples). Even in the case of H_2 uptake (Fig. 5(g) and (h)), based on the dataset reported by
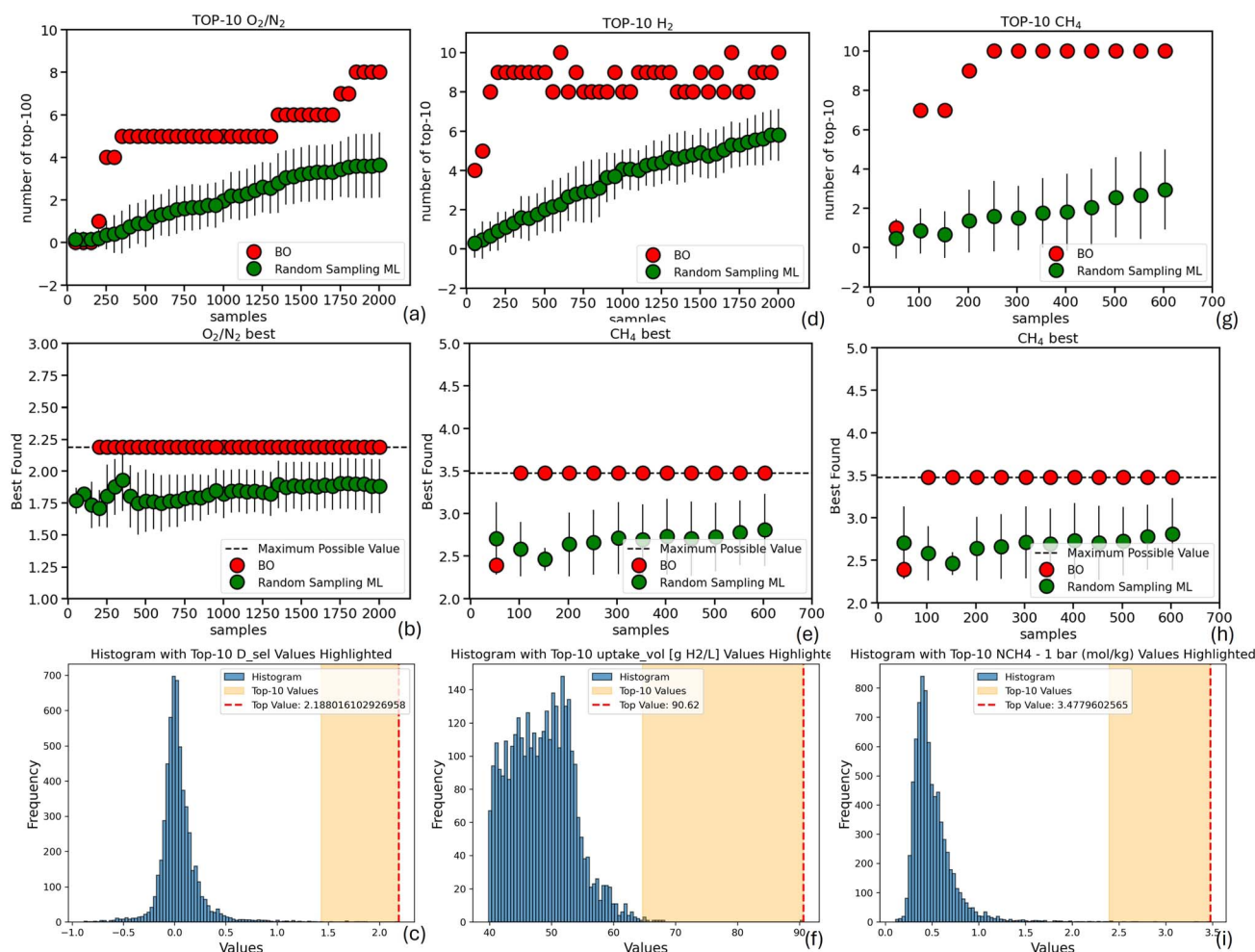

Fig. 7 Comparison of Bayesian Optimization (BO) and Random Sampling ML across three target properties: O_2/N_2 selectivity ((a)−(c)), H_2 uptake ((d)−(f)), and CH_4 uptake ((g)−(i)). (top row) Number of top-10 performing materials identified as a function of sample size. (middle row) Number of samples required to identify the top-1 performing material. (bottom row) Distribution of target property values across each dataset, providing context on the difficulty of each search task. Each plot compares the performance of BO and random sampling, illustrating the relative effectiveness of each approach in different regimes.

Majumdar *et al.*,[29] where random sampling shows a comparable ability to BO in identifying top-100 materials after approximately 1000 samples, it fails to identify the best-performing MOF—even after 2000 samples—highlighting the greater efficiency of the BO strategy. Again, the nDCG values of BO remain consistently higher than those of random sampling across all three cases (Fig. S3), highlighting BO's superior ability not only to identify the region containing the top-performing materials, but also to rank them in a manner that more closely reflects their true performance.

The same strong performance in identifying top-performing MOFs is observed when our BO method is applied to the three datasets reported by Majumdar *et al.*,[29] targeting CO_2 working capacity, CO_2/N_2 selectivity, and CO_2 uptake (Fig. 6). We draw the reader's attention particularly to the case of CO_2/N_2 selectivity, where the underlying distribution illustrates the difficulty of the task. Despite this challenge, BO achieves significantly higher identification performance and successfully discovers the best-performing MOF early in the search process. Once again, the nDCG values for BO are considerably higher than those for random sampling (Fig. S3), further demonstrating its superior ranking capabilities.

Finally, Fig. 7 presents the results for three additional datasets: O_2/N_2 diffusion selectivity in MOFs (from Orhan *et al.*[28]), H_2 uptake in MOFs (from Villajos *et al.*[31]), and CH_4 uptake in COFs (from Aksu and Keskin[2]). Due to the relatively smaller size of these datasets, we focused on the identification of the top-10 performing materials, reducing the evaluation threshold by an order of magnitude compared to previous cases. Even under this more stringent setting, our BO approach consistently outperforms random sampling, both in terms of identifying top performers and in ranking them effectively. BO successfully identifies a greater portion of the top-10 candidates with fewer samples, and—as confirmed by the nDCG scores—produces rankings that more closely reflect the true order of performance.

4 Conclusions

We have presented a frugality-oriented Bayesian Optimization (BO) framework tailored to the practical needs of materials scientists seeking not just a single optimum, but an ensemble of top-*N* performers from vast design spaces of functionalized nanoporous materials. By integrating three practical elements—(i) a diversity-preserving initialization scheme, (ii) batch-mode acquisitions to reduce retraining overhead, and (iii) a surrogate enrichment step in which an XGBoost model is trained on BO-acquired samples to predict and rerank the remainder of the space—we achieve a data-efficient workflow that dramatically reduces the number of expensive evaluations required. Across eight literature-derived datasets (MOFs and COFs spanning adsorption, diffusion, and selectivity targets), our BO framework recovers up to 2×–5× more true top-*N* candidates than a conventional ML pipeline trained on random samples (as measured by recall@*N*), and produces more accurate rankings (nDCG). Moreover, our BO method locates the single best performer with just 100–200 evaluations, whereas the random-sampling approach often still fails to find it after 2000 samples. By prioritizing task-specific metrics (recall@*N*, nDCG) over global measures (*e.g.*, R^2, MSE), we directly address the experimental goal of discovering rare, high-value materials under strict budget constraints. It is worth mentioning, in general, when comparing BO and Random Sampling ML, that BO is by construction a sequential process, whereas random sampling allows fully independent evaluations. In principle, if very large-scale parallel evaluation were available, random sampling could exploit this more directly and achieve faster turnaround despite lower sample efficiency. In practice, however, such scenarios remain largely hypothetical in materials discovery, where evaluations are typically costly and parallel resources are limited. Under these realistic conditions, BO provides a clear advantage by reducing the total number of evaluations required. The result is a robust and practical workflow—effective across diverse chemistries and objectives, and built entirely on standard Gaussian process and XGBoost tools. While our benchmarking focused on Random-Sampling ML as a baseline—reflecting its widespread use in prior literature and practice—we note that other strategies, such as uncertainty-based or diversity-driven active learning,[11] have also been explored for chemical design spaces. Incorporating such baselines in future work would provide additional perspective, but our present goal was to highlight the benefits of useful extensions to BO relative to the most common ML pipeline.

We envisage several concrete extensions to further enhance our framework's practical utility. First, integrating multi-objective BO methods—such as those by Kim *et al.*[32] and Hoang *et al.*[33]—would enable simultaneous optimization of multiple performance criteria (*e.g.*, selectivity *vs.* capacity). Second, replacing the Gaussian process surrogate with alternative probabilistic models (*e.g.*, Bayesian Neural Networks[34] or Gradient Boosting models with uncertainty estimation[35]) could alleviate the computational and scaling limitations of GPs. Third, human-in-the-loop strategies, as in HypBO,[36] would allow domain experts to steer the sampling process in real time, potentially accelerating convergence in difficult regions. Finally, minimizing the effective design space—following the ZoMBI algorithm of Siemenn *et al.*[17] —offers a promising route to reduce memory overhead, runtime, and the number of required samples, thereby addressing both the computational and the sampling costs. We are actively exploring these directions, though detailed implementation lies beyond the scope of this work.

Author contributions

Panagiotis Krokidas: conceptualization, formal analysis, methodology, software, supervision, writing; Vassisis Gkatsis: data curation, methodology, software, writing; John Theocharis: conceptualization, methodology, software; George Giannakopoulos: supervision, writing, methodology.

Conflicts of interest

There are no conflicts to declare.

Data availability

The codes for our (a) Bayesian optimization implementation as described in this manuscript and (b) the evaluation metrics estimation underlying this work are freely available for general use under the Apache License 2.0. They are deposited at https://github.com/insane-group/BO_for_Design_Space_Exploration and archived on Zenodo with DOI: https://doi.org/10.5281/zenodo.17491026. The datasets used in this work were obtained from literature, as cited in this manuscript.

Supplementary information: details of the XGBoost and Gaussian process models, comparison of efficient *vs.* random initialization, batch sampling performance, additional R^2, MSE and nDCG analyses, and computational setup used in this work. See DOI: https://doi.org/10.1039/d5dd00237k.

Acknowledgements

Notes and references

1 R. Batra, C. Chen, T. G. Evans, K. S. Walton and R. Ramprasad, *Nat. Mach. Intell.*, 2020, **2**, 704–710.
2 G. O. Aksu and S. Keskin, *J. Mater. Chem. A*, 2023, **11**, 14788–14799.
3 Y. He, E. D. Cubuk, M. D. Allendorf and E. J. Reed, *J. Phys. Chem. Lett.*, 2018, **9**, 4562–4569.
4 Z. Zheng, O. Zhang, C. Borgs, J. T. Chayes and O. M. Yaghi, *J. Am. Chem. Soc.*, 2023, **145**, 18048–18062.
5 Y. Kang and J. Kim, *Nat. Commun.*, 2024, **15**, 1–13.
6 A. S. Fuhr and B. G. Sumpter, *Front. Mater.*, 2022, **9**, 1–13.
7 A. Nandy, C. Duan and H. J. Kulik, *Curr. Opin. Chem. Eng.*, 2022, **36**, 100778.
8 R. Chang, Y. X. Wang and E. Ertekin, *npj Comput. Mater.*, 2022, **8**, 242.
9 B. Zong, J. Li, T. Yuan, J. Wang and R. Yuan, *J. Materiomics*, 2025, **11**, 100916.
10 F. Di Fiore, M. Nardelli and L. Mainini, *Arch. Comput. Methods Eng.*, 2024, **31**, 2985–3013.
11 A. Jose, E. Devijver, N. Jakse and R. Poloni, *J. Am. Chem. Soc.*, 2024, **146**, 6134–6144.
12 H. Liu, B. Yucel, B. Ganapathysubramanian, S. R. Kalidindi, D. Wheeler and O. Wodo, *Digital Discovery*, 2024, **3**(10), 1997–2009.
13 J. Schrier, A. J. Norquist, T. Buonassisi and J. Brgoch, *J. Am. Chem. Soc.*, 2023, **145**, 21699–21716.
14 S. R. Chitturi, A. Ramdas, Y. Wu, B. Rohr, S. Ermon, J. Dionne, F. H. Jornada, M. Dunne, C. Tassone, W. Neiswanger and D. Ratner, *npj Comput. Mater.*, 2024, **10**, 1–12.
15 Y. Wu, A. Walsh and A. M. Ganose, *Digital Discovery*, 2024, **3**, 1086–1100.
16 T. Loutas, A. Oikonomou and C. Rekatsinas, *Compos. Struct.*, 2025, **351**, 118597.
17 A. E. Siemenn, Z. Ren, Q. Li and T. Buonassisi, *npj Comput. Mater.*, 2023, **9**, 92.
18 T. Chen and C. Guestrin, *Proceedings of the 22nd ACM SIGKDD International Conference on Knowledge Discovery and Data Mining*, New York, NY, USA, 2016, pp. 785–794.
19 N. Gantzler, A. Deshwal, J. R. Doppa and C. M. Simon, *Digital Discovery*, 2023, **2**, 1937–1956.
20 M. Balandat, B. Karrer, D. R. Jiang, S. Daulton, B. Letham, A. G. Wilson and E. Bakshy, *Adv. Neural Inf. Process. Syst.*, 2020, **33**, 21524–21538.
21 M. Haddadnia, L. Grashoff and F. Strieth-Kalthoff, *Digital Discovery*, 2025, 1417–1422.
22 A. Deshwal, C. M. Simon and J. R. Doppa, *Mol. Syst. Des. Eng.*, 2021, **6**, 1066–1086.
23 F. Pedregosa, G. Varoquaux, A. Gramfort, V. Michel, B. Thirion, O. Grisel, M. Blondel, P. Prettenhofer, R. Weiss, V. Dubourg, J. Vanderplas, A. Passos, D. Cournapeau, M. Brucher, M. Perrot and E. Duchesnay, *J. Mach. Learn. Res.*, 2011, **12**, 2825–2830.
24 S. M. Moosavi, A. Nandy, K. M. Jablonka, D. Ongari, J. P. Janet, P. G. Boyd, Y. Lee, B. Smit and H. J. Kulik, *Nat. Commun.*, 2020, **11**, 1–10.
25 R. Mercado, R. S. Fu, A. V. Yakutovich, L. Talirz, M. Haranczyk and B. Smit, *Chem. Mater.*, 2018, **30**, 5069–5086.
26 D. Ginsbourger, R. L. Riche and L. Carraro, A Multi-points Criterion for Deterministic Parallel Global Optimization based on Gaussian Processes, *Institut National Polytechnique de Grenoble Technical Report hal-00260579*, 2008.
27 D. Ginsbourger, R. L. Riche and L. Carraro, *Computational Intelligence in Expensive Optimization Problems*, Springer, Berlin, Heidelberg, 2010, vol. 2, pp. 131–162.
28 I. B. Orhan, H. Daglar, S. Keskin, T. C. Le and R. Babarao, *ACS Appl. Mater. Interfaces*, 2022, **14**, 736–749.
29 S. Majumdar, S. M. Moosavi, K. M. Jablonka, D. Ongari and B. Smit, *ACS Appl. Mater. Interfaces*, 2021, **13**, 61004–61014.
30 V. Daoo and J. K. Singh, *ACS Appl. Mater. Interfaces*, 2024, **16**, 6971–6987.
31 J. A. Villajos, M. Bienert, N. Gugin, F. Emmerling and M. Maiwald, *Mater. Adv.*, 2023, **4**, 4226–4237.
32 J. Kim, M. Li, Y. Li, A. Gómez, O. Hinder and P. W. Leu, *Digital Discovery*, 2023, **3**, 381–391.
33 K. T. Hoang, S. Boersma, A. Mesbah and L. S. Imsland, *Renewable Energy*, 2025, **247**, 122988.
34 Y. L. Li, T. G. Rudner and A. G. Wilson, *12th International Conference on Learning Representations*, ICLR, 2024.
35 T. Duan, A. Avati, D. Y. Ding, K. K. Thai, S. Basu, A. Ng and A. Schuler, *37th International Conference on Machine Learning, ICML 2020*, 2020, PartF168147-4, pp. 2670–2680.
36 A. Cissé, X. Evangelopoulos, S. Carruthers, V. V. Gusev and A. I. Cooper, *Proceedings of the Thirty-Third International Joint Conference on Artificial Intelligence (IJCAI-24)*, 2024, pp. 3881–3889.